Materials and Design 104 (2016) 292–297

Contents lists available at ScienceDirect

Materials and Design

journal homepage: www.elsevier.com/locate/matdes

A study on diamond grinding wheels with regular grain distribution using additive manufacturing (AM) technology

Zhibo Yang *, Mingjun Zhang, Zhen Zhang, Aiju Liu, RuiYun Yang, Shian Liu

Henan Polytechnic University, Jiaozuo 454000, China

ARTICLE INFO

Article history:
Received 22 January 2016
Received in revised form 27 April 2016
Accepted 28 April 2016
Available online 7 May 2016

Keywords:
Interfacial microstructure
Diamond grinding wheel
3D printing
Ni-Cr alloy
Grinding performance

ABSTRACT

In this paper, a metal bound diamond grinding wheel with a regular grain distribution was fabricated based on 3D printing technology, which provides a solution to the irregular grain distribution and complicated preparation processes of diamond grinding wheels for use in precise/ultraprecise grinding. A grinding wheel was designed in 3D with pro/E, and the data transformation to the stereo-lithography format was carried out. The fabrication of the diamond grinding wheel was achieved with Ni-Cr alloy and diamond by 3D printing and sintering layer by layer. Scanning Electron Microscopy (SEM), Energy Dispersive Spectrometry (EDS) and X-ray diffraction (XRD) were employed to characterize the grains and the micro-structures between the substrate and the Ni-Cr alloy in the diamond grinding wheel, suggesting the infiltration mechanism of Ni-Cr towards the diamond and steel substrate. Finally, the grinding performance was evaluated with an experiment. It was shown that the abrasion of the diamond grinding grains was normal, and no grains fell off the wheel.

1. Introduction

With the development of high-speed and precise grinding, ceramic and resin binding grinding wheels have been unable to meet the requirements of modern production in the past several years. Therefore, the demand for diamond grinding wheels is becoming higher and higher [1–3]. Metal-binding grinding wheels have been widely applied to ceramic, optical glass, hard alloy and other materials, but with challenging preparation, due to their excellent performance in holding force, binding, abrasion, molding, life span, and grinding press bearing together with high precision and efficiency [4–8].

For current diamond grinding tools, the distribution of diamond grains in the metal matrix is random with segregation and aggregation. This has caused the grinding artifacts to have poor surface morphologies, low grinding efficiency, and short lives. In the diamond-abundant regions, the concentration of grinding grains is higher so that the grinding is weak and easily blocked, lowering the grinding efficiency, while in the diamond rare region, the concentration of grinding grains is low so that the grains are not involved in the grinding, which leads to the fracture and dropping of the grinding wheel caused by the overload and higher impact forces. The problems caused by uneven distribution of diamond grains cannot be ignored because of the vicious cycle they create [7,8]. Previous studies have reported regular distribution of grains using different methods and shown that regular distribution of grains can improve surface roughness, life span of the wheel, and grinding efficiency. Nevertheless, some issues still exist: namely, the complicated manufacturing process and high cost. Also, a regular distribution of grains can be realized in one dimension, but is difficult to achieve in 3 dimensions. There is therefore an urgent need for a process to manufacture wheels with regularly distributed diamond grains at a low cost [9–17].

3D printing technology is a booming industry that is beginning to change the style of manufacturing and living [18,19]. It is believed that new technologies like 3D printing with the features of digitization, network, personality and customization will lead to the 3rd industrial revolution [20–26]. 3D printing technology works by dividing a CAD mold into several layers in the computer and sintering or bonding plastic, metal powder, or even biological tissues or cells in a 3D CAD plane with the printing instrument layer by layer to form a 3-dimensional object [27]. 3D printing technology shows great potential as a direction of advanced technological development. It is crucial to fabricate diamond wheels with regular distribution grains due to the progress of grinding technology and the demand for application. In the present paper, a 3D printing method to fabricate end face diamond wheels with regularly distributed grains has been developed. The analysis of the micro-structures between the two different phases (diamond grains and Ni based alloy, and Ni based alloy and steel substrate) together with tracking observations of the performance of the end face diamond wheel grains have suggested explanations for the abrasion, which provides the experimental basis for the fabrication of diamond grinding wheel with regular distribution grains. Manufacturing this type of product is virtually impossible by conventional methods [21–27].

* Corresponding author.
E-mail address: Yangzhibo2001@163.com (Z. Yang).

http://dx.doi.org/10.1016/j.matdes.2016.04.104
0264-1275/

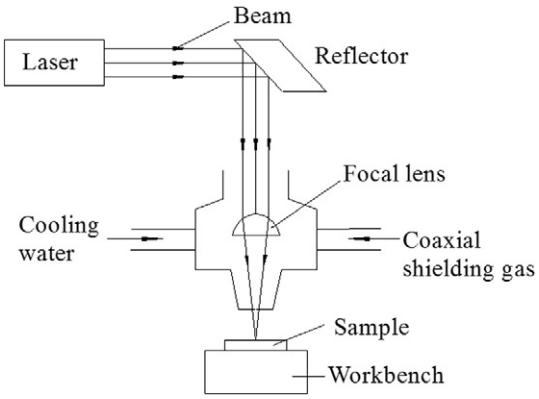

Fig. 1. Schematic of 3D printing instrument.

2. Instruments and methods

2.1. Materials and instruments

The grinding materials for the experiment were as follows: diamond, (size, 300–500 μm); metal binding powder (Ni_{75}-Cr_{18}-B_2-Si_5 alloy, self-made), with melting point 1000–1500 °C ; and substrate of AISI 1045 steel. The grinding wheel is a diamond wheel with an end face that is printed on the substrate ground and ultrasonically cleaned in acetone.

Instruments: TJ-HL-T5000 cross-flow CO_2 CNC laser machine. The initial laser mode is TEM00. The schematic for the 3D printing instrument is shown in Fig. 1.

The laser beam was originally a TEM00 (Transverse Electro – Magnetic) mold. In order to investigate the effects of 3D printing under different process parameters, the supplied energy density "ρ" was introduced in this paper.

$$\rho = P/bv$$

where ρ = supplied energy density (J/mm^2), P = laser power (W), b = width of laser spot (mm), and v = scanning speed (mm/s). The different results of laser printing under different process parameters were described by supplied energy density.

2.2. 3D model construction of diamond grinding wheel

A 3D model of a diamond grinding wheel was constructed using pro/E (Fig. 2). The model was divided into several layers by the software, allowing the cross-section image for each layer to be obtained. Multi-point data acquisition was then completed from the profile of the wheel together with the regular grains so that the printing route could be generated. This formed the 3D printing file (stereo-lithography, or STL).

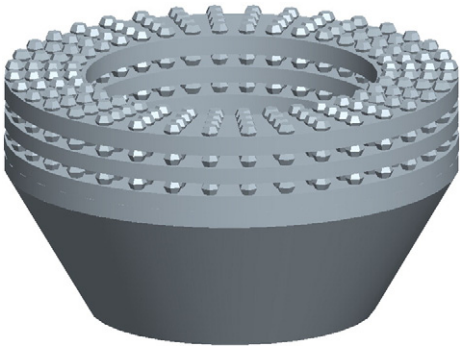

Fig. 2. Entity model of diamond grinding wheel.

2.3. 3D printing of the diamond grinding wheel

The STL file, which was generated from pro/E, was inputted into the 3D printer. The cross-section information of the grinding wheel was then transformed into a printing route by the printer. The 3D printing involved combined laser sintering and melting with laser fast scanning molding technology in order to obtain the target object. The preparation process for the diamond grinding wheel with regular distribution grains follows.

First, the mixture of Ni-Cr alloy powder and diamond grains was sprayed on the ASAI 1045-steel substrate uniformly by feeding devices.

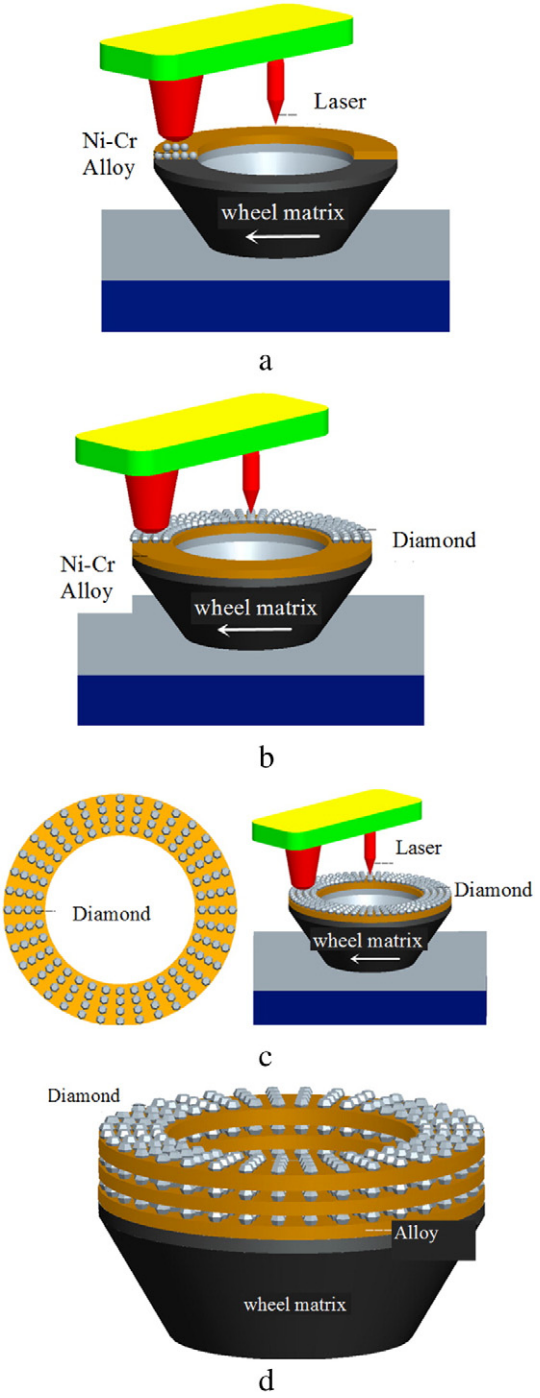

Fig. 3. 3D printing process of diamond grinding wheel with regularly distributed grains. a- Ni based binder 3D printer; b- Uniform spray of diamond grains; c- Regular distribution of grains; d- Diamond grinding wheel with regularly distributed grains.

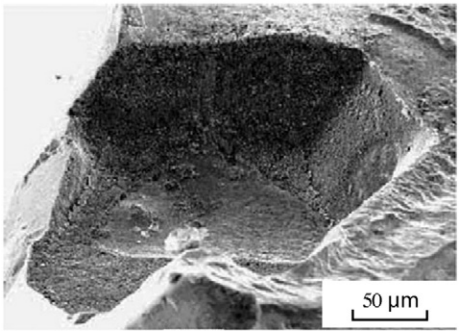

Fig. 4. Hole in filler surface.

Then, a CO_2-CNC laser machine would sinter and melt the Ni-Cr powder with the metal binder to proceed with material adding in a calculated route (Fig. 3a), and the diamond grinding grains could be sintered on the alloy with a binder in a way that is tightly controlled by a computer program (Fig. 3b). The power input was 300–500 W, the scanning speed was 25–35 mm/min, and the size of the beam was 3 mm × 2 mm. The laser energy is distributed in a rectangular area.

Any additional grains would be removed by the airflow so that a grinding wheel with regularly distributed diamond grains was produced (Fig. 3c). Finally, the procedure was repeated, as shown in Fig. 3a. Thus, a multi-layered grinding wheel with regularly distributed grains was fabricated after the materials were added layer by layer and the cooled to a solid state (Fig. 3e).

After 3D printing, the selected samples were cut, mounted and polished for evaluation of the interfacial microstructure between the grits and the alloy. JSM-6300 (JEOL) scanning electron microscopy (SEM) was employed to characterize the overall and lateral morphologies of the specimen after serious corrosion. Line scanning was performed by an Energy Dispersive Spectrometer (KEVEX, US). This scanning was used for the analysis of the element distribution of the Ni-Cr alloy cross-section. The composition of the carbonate on the diamond surface was determined by X-ray diffraction with Cu Kα radiation, operated at 40 kV and 40 mA. These measurements were carried out using a D'max (Rigaku, Japan).

3. Results and discussion

3.1. Features of 3D printed diamond grinding wheel

The orthogonal experiments were carried on based on tour previous parameters. Different results of laser printing under different process parameters are defined by the supplied energy density. If the supplied energy density is less than 342.8 J/mm^2, the diamond particles become dislodged while grinding on marble. An example is illustrated in Figs. 4 and 5, where solder balls can be seen in the resulting hole. If the supplied energy density is more than 364.2 J/mm^2, the diamond particles become graphitized, as can be seen in Figs. 6 and 7. The

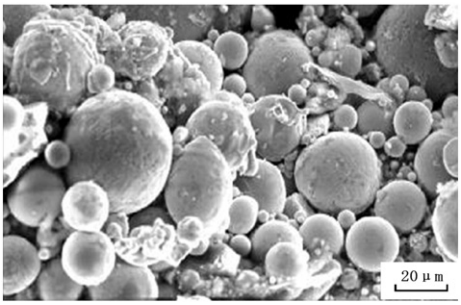

Fig. 5. Un-melted filler alloy.

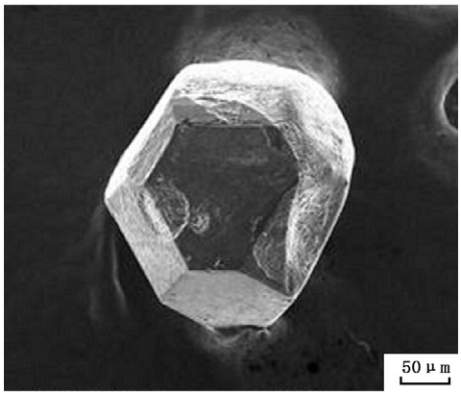

Fig. 6. Graphitized diamond.

substances in the surface of the diamond are flocculent if we amplify the graphitized area. (See Fig. 5.)

If ρ was more than 364.2 J/mm^2, the diamond grains would be graphitized (see Fig. 6). The resultant surface of the diamond is flocculent if we amplify the graphitized area (see Fig. 7).

If the supplied energy density is between 342.8 and 364.2 J/mm^2, a stronger 3D printed diamond results. Fig. 8 shows the combined morphology of the Ni-Cr alloy and the diamond particles after laser printing. A phenomenon can be observed that much crescent Ni-Cr alloy coated on the diamond grain edge. Obviously, the wetting of Ni-Cr alloy to diamond is good, and there could be some reactions between the Ni-Cr alloy and the diamond grain. In addition, there are no cracks or thermal damage on the diamond surfaces, and the shapes of diamond particles are intact. Figs. 9 and 10 show the integrate and local

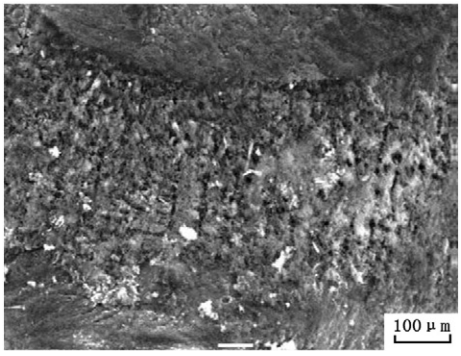

Fig. 7. Local amplification images.

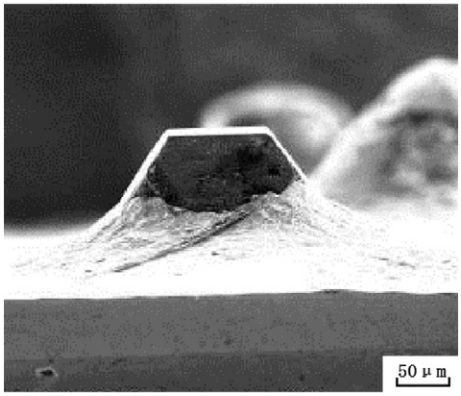

Fig. 8. SEM image of the 3D printing diamond grinding wheel.

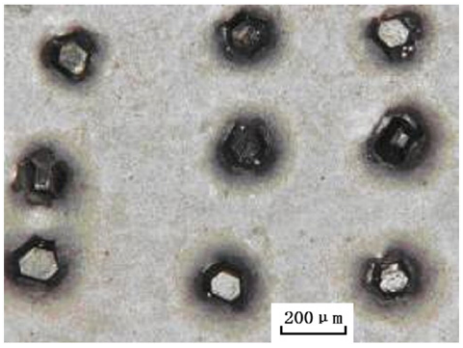

Fig. 9. Local morphology of the 3D printed diamond grinding wheel.

morphology of a diamond grinding wheel that was produced according to the procedures outlined in this study.

When the 3D printed process was finished, one sample was cut along the bonding interface, and subsequently the diamond grains were separated from the specimens by means of dissolving the filler layer in the 65% nitric acid. Ordered laser scanning sintering was shown to result in reaction products with tangential growth on the surface of the diamond grains, which can be observed in the SEM image of the diamond grains (Fig. 11). As shown from the XRD pattern (Fig. 12), these products are chromium carbides. In the reaction system between the diamond and the Ni substrate alloy, the concentration of Cr is the highest in the Ni-Cr alloy, suggesting its high activity involvement in the reactions. According to the previous study, Cr-C reaction is a type of diffusion reaction. In terms of thermodynamics, the standard free energy is $\Delta G0 = -71{,}555$ GJ/mol in the reaction in which Cr and C produce Cr_3C_2 at 1050 °C. The low standard free energy indicates that the formation of compounds between Cr and C is very easy. As for the diamond-metal system, the experiments revealed that chromium carbide can also be produced on the surface of diamond grains after a period of reaction due to the diffusive concentration gradient of carbon [9].

3.2. The combination between Ni-Cr alloy and steel substrate

The sample was cut off of the post-sintering Ni-Cr substrate and treated with coarse grinding, fine grinding and polish. The morphology of the interface between the substrate and the alloy was characterized by SEM (Fig. 13), and the composition of the interface was determined by EDS (Fig. 14).

As shown in Fig. 10, the concentration gradients of Ni, Cr, Si and Fe exhibited a slow transition trend, which indicates that the diffusion phenomena of the elements on both sides of the interface led to the formation of an alloy. During the laser sintering and molding process, mutual diffusion between the Ni-Cr alloy and the steel substrate took place at the laser temperature to form a solid phase diffusion zone. When the composition of the solid phase reached the composition of

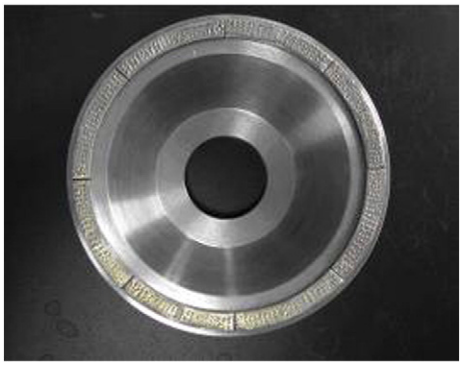

Fig. 10. Integrate morphology of the 3D printed diamond grinding wheel.

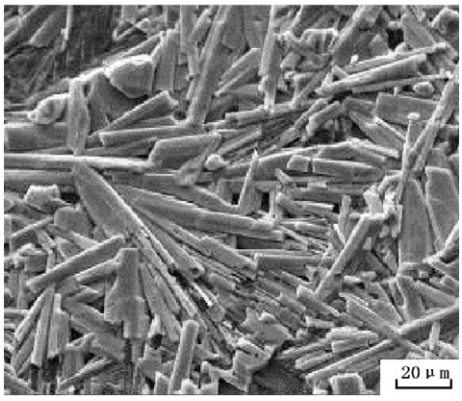

Fig. 11. Morphology of the product on the diamond surface.

eutectic point, liquid appeared due to the melting of the Ni-Cr alloy and the steel substrate on the interface. During the cooling process that followed, the Ni-Cr alloy and the steel substrate crystallized into a solid solution and compound so that the high-strength combination of Ni-Cr alloy and ASAI 1045-steel substrate could be produced.

4. Grinding test

In order to test the grinding performance of the fabricated diamond grinding wheel, inspection of the damage degree of the grinding grains under heavy loading was conducted. The conditions of the test are listed in Table 1.

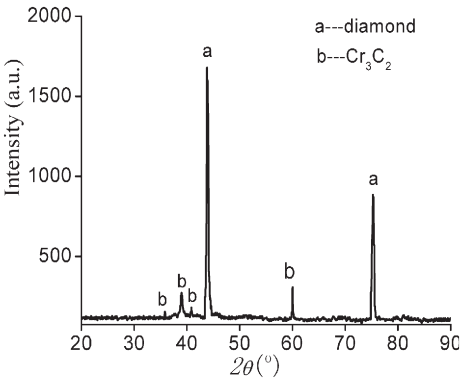

Fig. 12. XRD pattern of the diamond after laser scanning sintering.

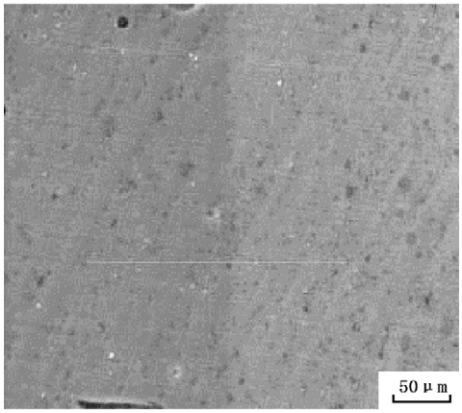

Fig. 13. SEM image of the interface between the substrate and the alloy.

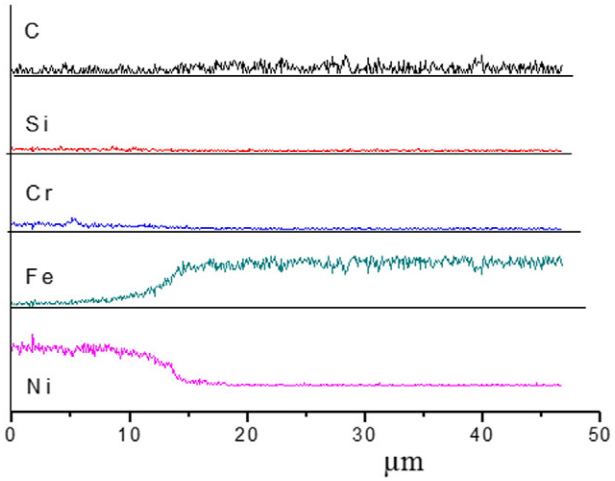

Fig. 14. Line scanning of the Ni-Cr interface.

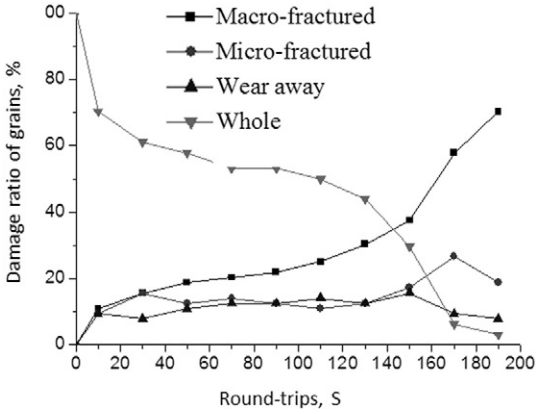

Fig. 16. Statistic analysis of morphological variation.

The diamond grains experienced different grinding morphologies from the start of the test to the failure of the wheel, which were observed by 3D video microscopy. After several grinding processes, the morphological changes of the cutting edges on the grains can be compared. Based on experimental observation. Fig. 15 shows the tracing morphological observation of a single diamond grain through the grinding process. Three main abrasion phenomena during the whole grinding process ware wear-away, micro-fractured, and macro-fractured without grain dropping. During the test, those grains displaying wear-away or micro-fractures were still usable in the grinding process, since the fractures actually created new cutting edges, benefitting the entire grinding process.

Statistical analysis of the morphology at particular times was used in the current experiment in order to understand the changing trend of the grinding grains. There were nearly 190 round processes during the whole test from the beginning of grinding to the failure of the grinding wheel. Proportions for several typical abrasive morphologies of grains during the round processes are presented in Fig. 16.

The grinding grains with regular distribution on the wheel experienced normal abrasion and breakage during the grinding process, which is a normal phenomenon in super-hard abrasive manufacture, without grain droppage.

5. Conclusions

1) With the assistance of 3D photographic software and computer control, a combination of 3D printing, laser molding with sintering and melting, and dynamic point scanning can be used for the preparation of diamond grinding wheels with regularly distributed grains.

2) It was shown that 3D printing can be extremely successful for grinding wheel fabrication because of its ability to control distribution of grains in 3 dimensions and multiple layers without sacrificing simplicity in the manufacturing process. On the prepared diamond grinding wheel, Cr-C compound was found on the interface of the

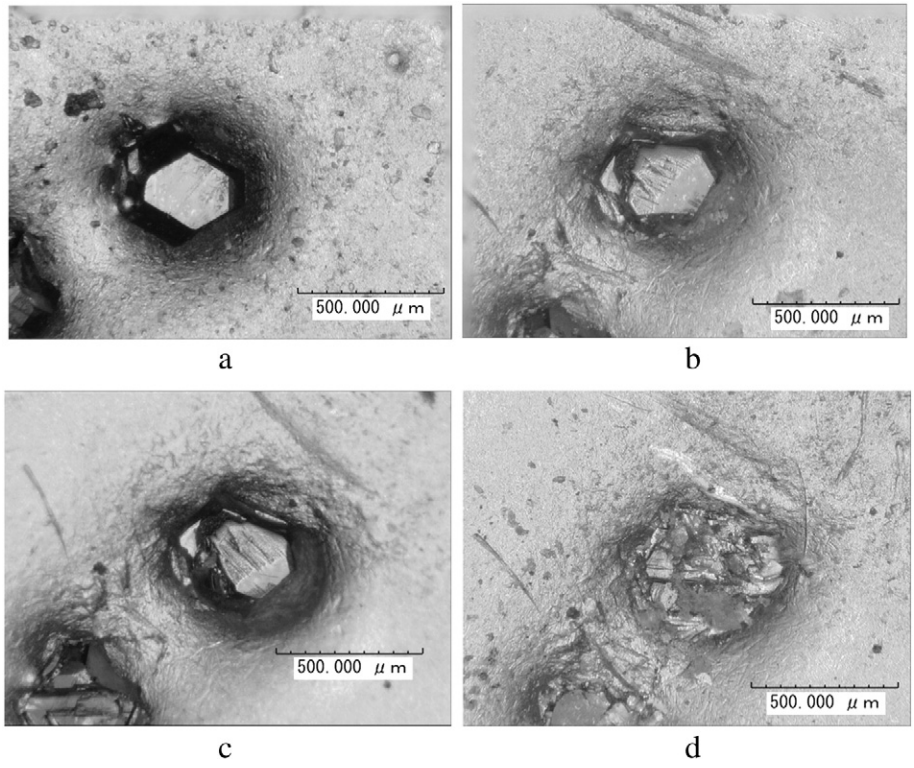

Fig. 15. The morphological change of a single diamond grain. a- overall morphology; b- wear-away morphology; c- Micro-fractured morphology; d- Macro-fractured morphology.

Table 1
Grinding test conditions for 3D printed diamond wheel.

Items	Conditions
Machine tool	MMD7125 precision surface grinding machine
Materials	Sichuan red granite (density: 2.58 g/cm^3, Xiao Hardness: HS 92)
Cooling mode	Water cooling Pressure at 0.4 MPa
Grinding mode	End face grinding
Loading method	Normal force measuring
Wheel speed vs/(m·s^{-1})	20
Workpiece speed vw/(m·min^{-1})	2
Depth of cut a_p/mm	0.08
Morphology observation	3D video microscope

diamond grains, which can strength the degree of binding between the metal binder and the diamond. A diffusion transfer region with good metallurgical bonding between the alloy and the substrate has been confirmed.

3) Under high-load grinding conditions, no dropping phenomenon appeared on the 3D printed diamond grinding wheel.

Acknowledgement

This research was supported by the financially by The National Natural Science Foundation of China(U1204517), Natural Science Fund by the Education department of Henan Province P.R. China (12B460011), the Opening Project of Key Laboratory of Precision Manufacturing technology and engineering, Henan Polytechnic University (PETM-9235).

References

[1] J.L. Li, C.H. Li, J.M. Guo, Research and development of metal bonded diamond grinding wheel, Tool Technol. 37 (2003) 3–6.
[2] Y.X. Sun, Y.T. Tsai, K.H. Lin, The influence of sintering parameters on the mechanical properties of vitrified bond diamond tools, Mater. Des. 80 (2015) 89–98.
[3] S. Goel, X. Luo, R.L. Reuben, W.B. Rashid, Replacing diamond cutting tools with CBN for efficient nanometric cutting of silicon, Mater. Des. 68 (2012) 507–509.
[4] M. Zeren, S. Karagöz, Sintering of polycrystalline diamond cutting tools, Mater. Des. 28 (2007) 1055–1058.
[5] J. Webster, M. Tricard, Innovations in abrasive products for precision grinding, Ann. CIRP 53 (2004) 597–617.
[6] A. Pilipovic, I. Drstvensek, M. Sercer, Mathematical model for the selection of processing parameters in selective laser sintering of polymer products, Adv. Mech. Eng. 6 (2014) 1–9.
[7] S. Daria, M.J. Leon, L. Evgeny, L. Pavel, P. Mikhail, Carbon nanotube reinforced metal binder for diamond cutting tools, Mater. Des. 83 (2015) 536–544.
[8] G.X. Mei, Q.L. Li, H.H. Su, J.H. Xu, Based on the brazing of abrasive orderly arranged diamond tool the new preparation technology research, Mach. Manuf. Autom. 4 (2012) 10–11.
[9] H. Gao, J.L. Liu, Composite electrodeposition ultra-thin diamond cutting disc grinding grain distribution uniformity, J. Mater. Sci. Eng. 4 (2010) 477–480.
[10] D. Sidorenko, L. Mishnaevsky, E. Levashov, P. Loginov, M. Petrzhik, Carbon nanotube reinforced metal binder for diamond cutting tools, Mater. Des. 83 (2015) 536–544.
[11] C. Heinzel, K. Rickens, Engineered wheels for grinding of optical glass, CIRP Ann. Manuf. Technol. 58 (2009) 315–318.
[12] Z. Fang, T.T. Zhao, C.H. Li, Optimization arrangement of diamond grits: a laser alignment technique and evaluation of the grinding force and the wear characteristics, Precis. Manuf. Autom. 1 (2011) 3–7.
[13] S.H. Yin, F.J. Chen, J.W. Yu, M. Wang, A novel orderly arrangement method controlled by magnetic field for diamond abrasives of grinding wheel, Adv. Mater. Res. 497 (2012) 6–9.
[14] B. Berman, 3D printing: the new industrial revolution, Bus. Horiz. 55 (2012) 155–162.
[15] C. Weller, R. Kleer, T. Frank, Economic implications of 3D printing: markets structure models in light of additive manufacturing revisited, Int. J. Prod. Econ. 164 (2015) 43–56.
[16] Y.P. Yang, Y. Liu, C.H. Song, Metal parts 3D printing technology present situation and research progress, Mech. Electr. Eng. 1 (2013) 1–12.
[17] F.J. Alan, Development of a valve-based cell printer for the formation of human embryonic stem cell spheroid aggregates, Biofabrication 1 (2013) 1–12.
[18] L. Pavel, M. Leon, L. Evgeny, M. Petrzhik, Diamond and CBN hybrid and nanomodified cutting tools with enhanced performance: development, testing and modelling, Mater. Des. 88 (2015) 310–319.
[19] Z.B. Yang, J.H. Xu, A.J. Liu, Analysis of microstructure of the interface of laser brazing diamond, Trans. China Weld. Inst. 31 (2010) 9–14.
[20] S. Goel, X. Luo, R.L. Reuben, Wear mechanism of diamond tools against single crystal silicon in single point diamond turning process, Mater. Des. 57 (2013) 272–281.
[21] B. Caulfield, P.E. McHugh, S. Lohfeld, Dependence of mechanical properties of polyamide components on build parameters in the SLS process, J. Mater. Process. Technol. 182 (2006) 477–488.
[22] Z. Guang, Z.Y. Han, S.M. Liang, P. Zhang, X.L. Chen, P.X. Zhang, Metal parts of 3D printing technology application research, China's Mater. Prog. 33 (2014) 377–382.
[23] S.F. Huang, H.L. Tsai, S.T. Lin, Laser brazing of diamond grits using a Cu-15Ti-10Sn brazing alloy, Mater. Trans. 43 (2002) 2604–2608.
[24] S.R. Maity, P. Chatterjee, S. Chakraborty, Cutting tool material selection using grey complex proportional assessment method, Mater. Des. 36 (2012) 372–378.
[25] Z.B. Yang, A.J. Liu, R.Y. Yang, Analysis of Laser-Brazed Diamond Particle Microstructures. Mater. Sci. 21 (4)
[26] V.I. Lavrinenko, G.D. Il'nitskaya, G.A. Petasyuk, V.N. Tkach, V.V. Smokvina, V.S. Shamraeva, I.N. Zaitseva, D.G. Muzychka, The influence of physical-mechanical characteristics of AS6 synthetic diamond powders on wear resistance of grinding tools, J. Superhead Mater. 35 (2013) 309–315.
[27] J. Bomo, F. Ezan, F. Tiaho, M. Bellamri, S. Langouet, N. Theret, G. Baffet, Increasing 3D matrix rigidity strengthens proliferation and spheroid development of human liver cells in a constant growth factor environment, J. Cell. Biochem. 17 (2016) 708–720.